

Studies of structural and electronic properties of InP layers formed by plasma-enhanced atomic layer deposition on a Si substrate with a GaP sublayer

© A.S. Gudovskikh^{1,2}, A.I. Baranov¹, A.V. Uvarov¹, E.A. Vyacheslavova¹, A.A. Maksimova^{1,2},
D.A. Kirilenko³, G.I. Yakovlev², V.I. Zubkov²

¹ Alferov Federal State Budgetary Institution of Higher Education and Science Saint Petersburg National Research Academic University of the Russian Academy of Sciences, St. Petersburg, Russia

² St. Petersburg State Electrotechnical University „LETI“, St. Petersburg, Russia

³ Ioffe Institute, St. Petersburg, Russia

E-mail: gudovskikh@spbau.ru

Received November 27, 2024

Revised January 4, 2025

Accepted January 10, 2025

The structural and electronic properties of InP layers and the GaP/InP interface formed by plasma-enhanced chemical atomic layer deposition on a Si substrate were studied. When InP was grown on a Si substrate with a GaP sublayer (20 nm), a sharp InP/GaP interface was observed and the properties of the GaP/Si interface were preserved. Measurements of the carrier concentration profiles using electrochemical CV profiling for the InP/GaP/Si heterostructure allowed us to estimate ΔE_C at the GaP/InP interface as 0.55 ± 0.05 eV.

Keywords: indium phosphide, gallium phosphide, interface, atomic layer deposition.

DOI: 10.61011/0000000000

Formation of multi-layer structures based on compounds A^3B^5 on a silicon substrate is of great interest for development of new optoelectronic devices, such as light-emitting, photo-detecting and photo-converting structures. To form a buffer layer grown on silicon, the optimal candidate among binary compounds A^3B^5 is GaP, having the least disagreement of the permanent crystalline lattice. However, to form photoactive layers, it is necessary to use direct-band compounds or multi-layer structures. In particular, quantum-size structures are used on the basis of a combination of InP and GaP layers. For such periodic InP/GaP structures on GaAs substrates, the possibility was shown previously to vary the width of the band gap in the range of 1.65 to 2 eV depending on the number of periods and the layer thicknesses [1,2]. Formation of quantum wells and quantum dots InP/GaP on the silicon substrates is of great interest for development of emitting structures integrated with silicon-based electronics [3–7]. On the other hand, microcrystalline InP layers with rather high values of charge carrier lifetime, formed on the silicon, are of interest for development of photovoltaic converters of solar energy as a photoactive layer of single-transition [8,9] or tandem structures when GaInP solid solutions or short-period InP/GaP-superlattices are formed [10]. For use in photovoltaic converters of solar emission, the technology of forming such devices should provide the possibility of large-scale production with minimal energy consumption, which may be provided by using thin-film technology of synthesis at comparatively low temperatures. Previously the possibility was demonstrated to grow InP and multi-layer InP/GaP-heterostructures using the method of plasma-chemical atomic layer deposition at

temperature 380 °C. However, in this case in association with InP growth on Si, the deterioration of the interface InP/Si was observed, with pits detected by transmission microscopy of high resolution on the silicon surface formed by Si etching in the process of InP layer growth [10]. This paper studied the properties of the interface in association with the plasma-chemical growth of InP layers on Si-substrate with the previously deposited GaP sublayer. This configuration is of great practical interest, since in the actual device structures the Si surface must contain a layer of a wide-band window to Si or a potential barrier to InP. It should also be noted that the plasma-chemical growth of GaP on the silicon and heteroboundary of GaP/Si have been studied quite well [11,12] and, therefore, the InP/GaP interface is of the greatest interest.

In the paper the GaP and InP layers were formed by the method of plasma-chemical atomic layer deposition on substrates of single-crystal Si with orientation (100) of *n*-type conductance with concentration of 10^{17} cm^{-3} . Immediately prior to deposition, Si-substrates were treated in 10 % HF aqueous solution to remove natural oxide and ensure hydrogen passivation. First the GaP sublayer was deposited on the Si surface, and then the InP layer was grown. An Oxford Plasmalab System 100 PECVD setup was used to perform deposition at a temperature of 380 °C and a pressure of 350 mTorr. Trimethylindium (TMI) and trimethyl gallium (TMG), respectively, were used as a source of In and Ga, and — phosphine (PH_3) was used as a source of phosphorus. Layer-by-layer growth was achieved by implementing the following cycle: decomposition of PH_3 in plasma of a radio-frequency (13.56 MHz) discharge with

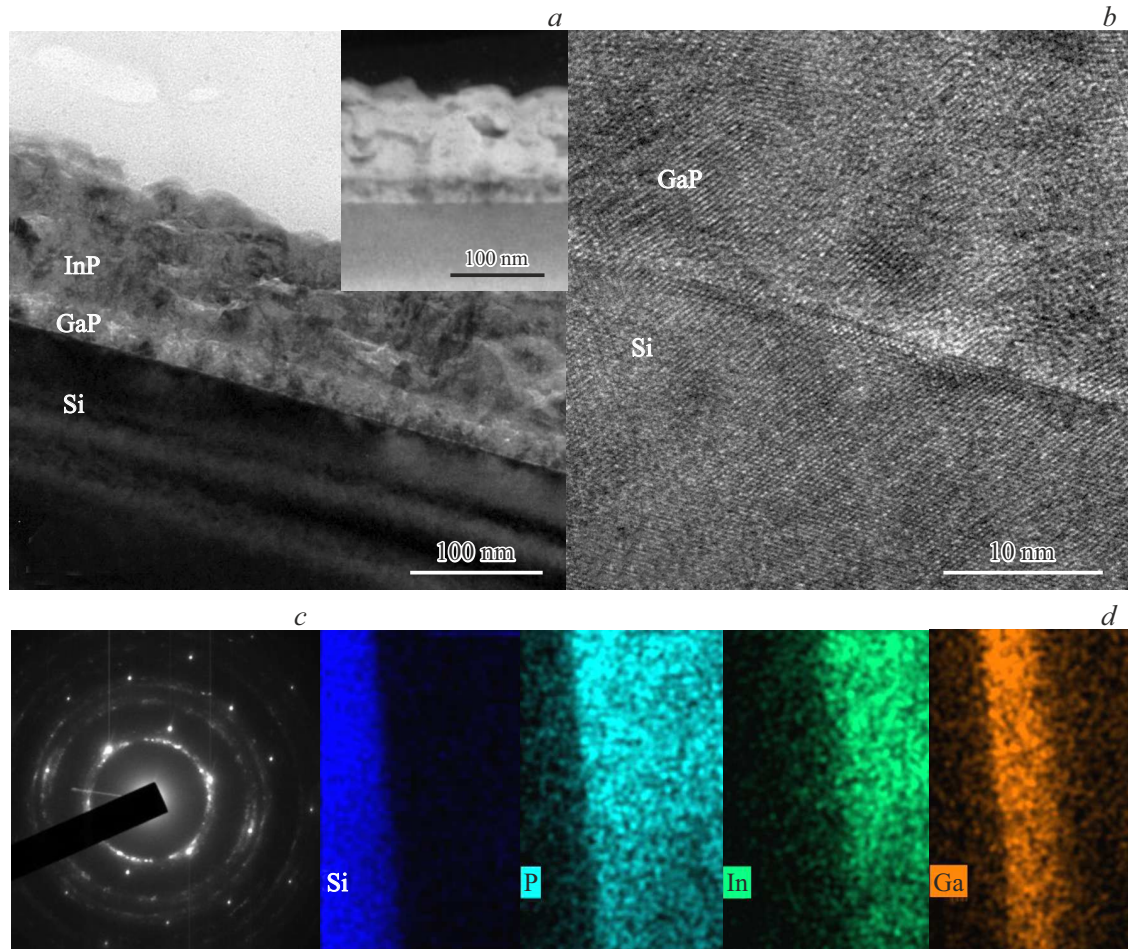


Figure 1. Microphotographs of GaP/InP-structure cross section on Si (a), obtained using TEM and HAADF-STEM (in the insert), of interface Si/GaP (b), the image of electron diffraction (c) and charts of main elements distribution obtained using energy-dispersive X-ray spectroscopy (d).

a power density of 90 mW/cm^2 ; purging with Ar; thermally activated surface reaction of metalorganic compounds TMI or TMG); purging with Ar. Plasma was ignited only at the stage of phosphorus deposition. The thickness of the formed GaP layer in the cycle process is equal to $0.10 \pm 0.01 \text{ nm}$, and the thickness of InP formed within a single cycle is $0.17 \pm 0.01 \text{ nm}$. The total thickness of GaP layer was 20 nm , and of InP layer — 100 nm . Additionally InP was deposited on a semi-insulating InP substrate for independent measurement of charge carrier concentration.

The structural properties of heterostructures were studied using transmission electron microscopy (TEM) (JEM-2100F microscope), as well as Raman spectroscopy using a laser at a wavelength of 532 nm (EnSpectr R532 spectrometer). According to the TEM results presented in fig. 1, GaP layers matched by crystalline lattice parameter to Si, demonstrate the initial epitaxial growth with transition to a microcrystalline structure. As the research shows, using a high-angle annular dark field transmission electron microscopy (HAADF-STEM) (insert in fig. 1, a) and high-resolution TEM (fig. 1, b), the Si/GaP interface is even, the silicon surface contains no etching pits observed in

direct growth of InP on Si [10]. InP layers grown on the GaP sublayer, similarly to InP layers grown on Si, have microcrystalline structure with weak preferential orientation (111), which is confirmed by TEM-image of cross section (fig. 1, a) and pattern of selected area electron diffraction (SAED) (fig. 1, c). The contrast on the TEM image in the light and dark field (fig. 1, a), and element distribution charts obtained using energy-dispersive X-ray spectroscopy (fig. 1, d), demonstrate the presence of the sharp boundary between the GaP and InP layers.

For InP layers grown on semi-insulating InP substrates ($\geq 10^7 \Omega \cdot \text{cm}$), the Hall effect was used to measure concentration and mobility of the charge carriers. Ohmic contacts in the geometry of Van der Pauw were formed on the surface of the InP layers. Measurements were done using installation Ecopia HMS-3000 with permanent magnet of 0.5 T . According to the measurements, the layers have n -type of conductance with electron concentration $(1-2) \cdot 10^{17} \text{ cm}^{-3}$ and mobility $1500-1700 \text{ cm}^2 \cdot \text{V}^{-1} \cdot \text{s}^{-1}$.

The electronic properties of the layers and heterostructures were studied using electrochemical capacitance-voltage (CV) profiling using profilometer ECVPro (Nano-

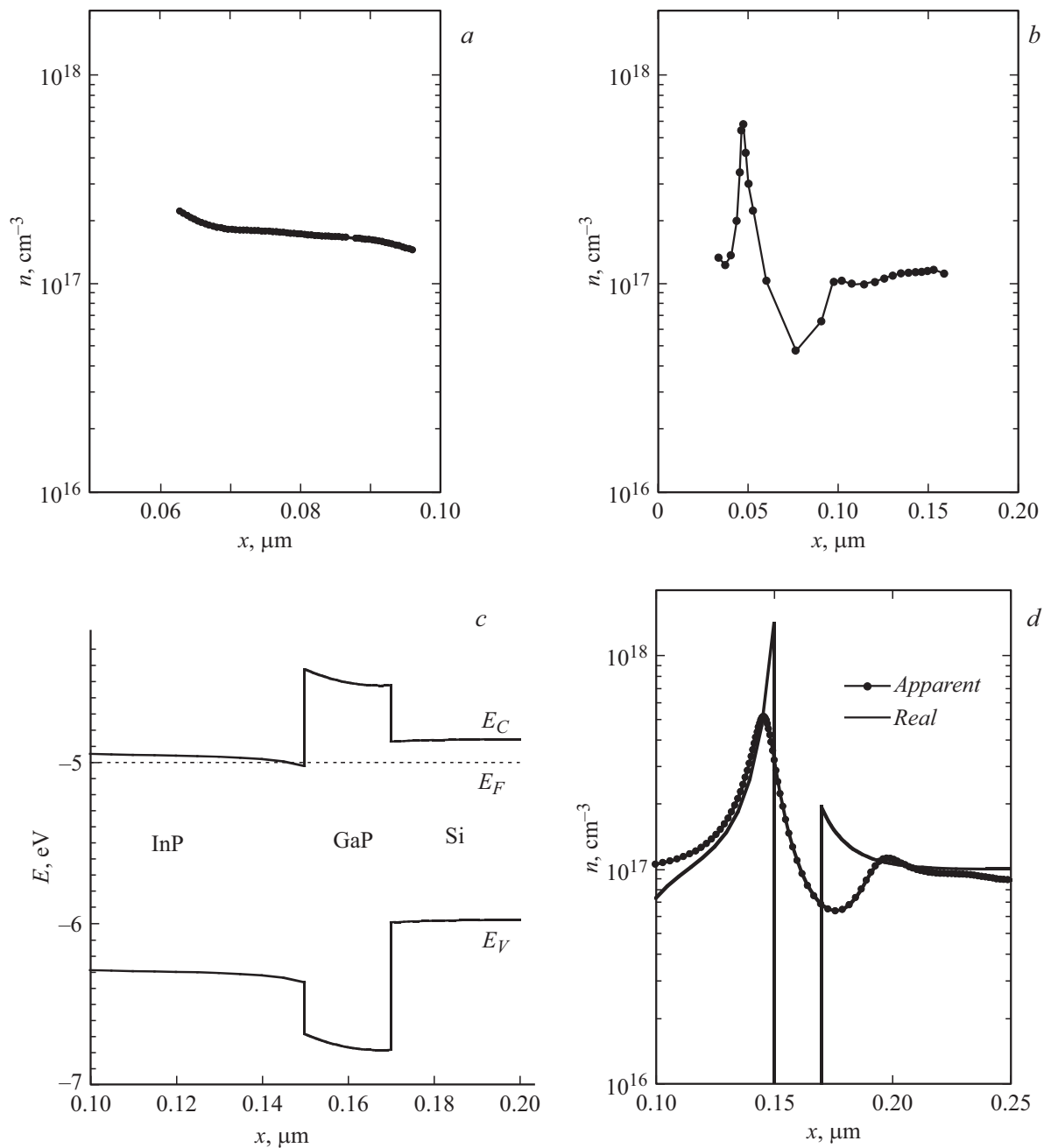


Figure 2. Measured profiles $n(x)$ for the InP layer grown on the InP substrate (a), and for InP/GaP/Si-heterostructure (b), the estimated band diagram of InP/GaP/Si-heterostructure (c) and its „observed“ and real profiles $n(x)$ (d).

metrics) and *RLC*-meter Agilent E4980A-001 in the profiling mode due to variation of the volume charge area width (without etching). The electrolyte was the solution NH_4HF_2 (0.2 M) with addition of surfactant Triton X-100, amplitude of test signal 100 mV, frequency 0.1–5 kHz, etching current 0.2–0.6 mA/cm². It should be noted that for the profiles obtained using *CV*-profiling, hereinafter referred to as „observed“ (i.e. in non-equilibrium conditions of the experiment), hardware blurring is specific, therefore they might differ from the real distribution of main charge carriers. Blurring of „observed“ concentration profiles

happens due to unclear boundary of volume charge area (VCA) specified by the Debye screening length [13]. The obtained profiles of charge carrier concentration are shown in fig. 2, a, b. For the InP layer grown on the semi-insulating InP substrate, the concentration of the charge carriers in the range of $(1.5\text{--}2) \cdot 10^{17}$ cm⁻³, is rather homogeneously distributed along the layer thickness (fig. 2, a). The produced values correspond to the electron concentration pretty much, and the concentration was determined using Hall effect, which indicates the validity of the completed measurements. The profile of the concentration of main

charge carriers in InP/GaP/Si-heterostructure (fig. 2, *b*) was made by superposition of local concentration profiles in the profiling mode due to variation of the VCR width measured at different etching depths [14]. The profile shows the area of electron accumulation, the subsequent area of depletion and constant concentration in substrate *n*-Si. This feature was fully reproduced at repeated measurements. The electron accumulation area corresponds to near surface area *n*-InP next to interface *n*-InP/*n*-GaP and is due to the band bending caused by conduction band break (ΔE_C) at this interface, as shown on the band chart in fig. 2, *c*. Therefore, the produced profile $n(x)$ may estimate quantitatively of band break ΔE_C . For this purpose, a numerical modeling was executed for the „observed“ profiles of charge carrier distribution, i.e. profiles determined using the CV-profiling method. In the estimate done by AFORS-HET software [15], the experimentally measured values were used for ΔE_C at the GaP/Si interface (0.35 eV [12]) and doping levels of InP layers ($1.5 \cdot 10^{17} \text{ cm}^{-3}$), GaP ($4 \cdot 10^{17} \text{ cm}^{-3}$) and Si-substrate (10^{17} cm^{-3}). Value ΔE_C at InP/GaP interface varied in the range of 0.2–0.8 eV. For the heterostructures *n*-InP/*n*-GaP/*n*-Si modeled, the surface *n*-InP created a bend of bands simulating the Schottky barrier, and the calculation of CV-characteristics was done. Using the calculated CV-characteristics, the „observed“ $n(x)$ distribution profiles were estimated under the procedure described in [13]. The best compliance with the experimental data is observed for ΔE_C , which are in the range of 0.5–0.6 eV. The real profile $n(x)$ and its corresponding „observed“ profile calculated for $\Delta E_C = 0.6 \text{ eV}$ are presented in fig. 2, *d*. The shift of the right boundary of the depletion region for the „observed“ $n(x)$ towards larger depths is related to the difference in the dielectric constant for the InP and GaP layers, which is not taken into account in the calculation. The calculated (fig. 2, *d*) and the experimental (fig. 2, *b*) „observed“ profiles $n(x)$ are in good quality and quantity compliance. Apart from the region of electron accumulation, the depletion region in the GaP layer is reproduced well too. The difference in the absolute values x is provided for by the preliminary etching of the InP layer prior to performance of CV-measurements. Similarly the profiles $n(x)$ measured using electrochemical CV-profiling were analyzed, for the structure with the quantum well InP, located between the barrier layers of GaP, grown by the method of metalorganic vapour phase epitaxy (MOC-hydride epitaxy) on the GaP substrate [16]. The estimate ΔE_C at the GaP/InP interface produced as a result of the analysis is $0.58 \pm 0.02 \text{ eV}$, which is in good agreement with the results presented above. The self-agreed calculation by the strong coupling method for GaP/InP provides the value $\Delta E_C = 0.55 \text{ eV}$ [17]. Using optical measurements of stressed InP/GaP-superlattices, the experimental estimate ΔE_C of around 0.3 eV is produced [18], however, later, using the results of research on the dependence of photoluminescence spectra on hydrostatic pressure for the structures with quantum dots InP/GaP, the values $\Delta E_C = 0.61 \pm 0.03 \text{ eV}$ were defined [19], which are very close to the results obtained in this study.

Therefore, it is shown that using a GaP sublayer on the Si surface in plasma-chemical atomic-layer deposition of InP layers makes it possible to form a clear interface of InP/GaP and maintain the surface of Si-substrate without formation of visible defects in contrast to the direct growth of InP on the Si surface. Measurements of charge carrier concentration profiles using electrochemical CV-profiling for *n*-GaP/*n*-InP/*n*-Si structures made it possible to estimate the break value of the conduction bands (ΔE_C) at the GaP/InP interface being $0.55 \pm 0.05 \text{ eV}$. The high value of ΔE_C is developed by the potential barrier for the electrons at the interface *n*-GaP/*n*-InP and, therefore, may impact their transport, which must be taken into account in development of photoconverters on the structures containing GaP/InP interfaces.

Funding

The study was supported by a grant from the Russian Science Foundation № 24-19-00150 (<https://rscf.ru/project/24-19-00150/>). The TEM studies were performed using the equipment of the federal Common Research Center „Materials Science and Diagnostics in Advanced Technologies“, supported by the Ministry of Education and Science of Russia.

Conflict of interest

The authors declare that they have no conflict of interest.

References

- [1] J.D. Song, Y.-W. Ok, J.M. Kim, Y.T. Lee, T.-Y. Seong, *J. Appl. Phys.*, **90** (10), 5086 (2001). DOI: 10.1063/1.1412267
- [2] S.J. Kim, K. Asahi, K. Asami, M. Takemoto, M. Fudeta, S. Gonda, *Appl. Surf. Sci.*, **130-132**, 729 (1998). DOI: 10.1016/S0169-4332(98)00145-7
- [3] R. Balasubramanian, V. Sichkovskiy, C. Corley-Wiciak, F. Schnabel, L. Popilevsky, G. Atiya, I. Khanoknin, A.J. Willoger, O. Eyal, G. Eisenstein, J.P. Reithmaier, *Semicond. Sci. Technol.*, **37** (5), 055005 (2022). DOI: 10.1088/1361-6641/ac5d10
- [4] M.-S. Park, M. Rezaeei, I. Nia, R. Brown, S. Bianconi, C.L. Tan, H. Mohseni, *Opt. Mater. Express*, **8** (2), 413 (2018). DOI: 10.1364/OME.8.000413
- [5] P. Dhirga, P. Su, B.D. Li, R.D. Hool, A.J. Muhowski, M. Kim, D. Wasserman, J. Dallesasse, M.L. Lee, *Optica*, **8** (11), 1495 (2021). DOI: 10.1364/OPTICA.443979
- [6] F. Hatami, W.T. Masselink, L. Schrottke, J.W. Tomm, V. Talalaev, C. Kristukat, A.R. Goñi, *Phys. Rev. B*, **67**, 08530610 (2003). DOI: 1103/PhysRevB.67.085306
- [7] F. Hatami, W.T. Masselink, J.S. Harris, *Nanotechnology*, **17**, 3703 (2006). DOI: 10.1088/0957-4484/17/15/014
- [8] R. Kapadia, Z. Yu, H.-H.H. Wang, M. Zheng, C. Battaglia, M. Hettick, D. Kiriya, K. Takei, P. Lobaccaro, J.W. Beeman, J.W. Ager, R. Maboudian, D.C. Chrzan, A. Javey, *Sci. Rep.*, **3**, 2275 (2013). DOI: 10.1038/srep02275

- [9] W. Metaferia, Y.-T. Sun, S.M. Pietralunga, M. Zani, A. Tagliaferri, S. Lourdudoss, J. Appl. Phys., **116**, 033519 (2014). DOI: 10.1063/1.4890718
- [10] A.S. Gudovskikh, A.V. Uvarov, A.I. Baranov, E.A. Vyacheslavova, A.A. Maksimova, D.A. Kirilenko, Semiconductors, **58** (2), 134 (2024). DOI: 10.1134/S1063782624020076.
- [11] A.V. Uvarov, A.S. Gudovskikh, V.N. Nevedomskiy, A.I. Baranov, D.A. Kudryashov, I.A. Morozov, J.-P. Kleider, J. Phys. D, **53**, 345105 (2020). DOI: 10.1088/1361-6463/ab8bfd
- [12] A.S. Gudovskikh, A.I. Baranov, A.V. Uvarov, D.A. Kudryashov, J.-P. Kleider, J. Phys. D, **55** (13), 135103 (2022). DOI: 10.1088/1361-6463/ac41fa
- [13] S.R. Forrest, in *Heterojunction band discontinuities: physics and device applications* (Elsevier, 1987), p. 311.
- [14] G. Yakovlev, V. Zubkov, J. Solid State Electrochem., **25**, 797 (2021). DOI: 10.1007/s10008-020-04855-0
- [15] R. Varache, C. Leendertz, M.E. Gueunier-Farret, J. Haschke, D. Muñoz, L. Korte, Solar Energy Mater. Solar Cells, **141**, 14 (2015). DOI: 10.1016/j.solmat.2015.05.014
- [16] A.I. Baranov, A.V. Uvarov, A.A. Maksimova, E.A. Vyacheslavova, N.A. Kalyuzhnyy, S.A. Mintairov, R.A. Salii, G.E. Yakovlev, V.I. Zubkov, A.S. Gudovskikh, Tech. Phys. Lett., **49** (Suppl. 3), S163 (2023). DOI: 10.1134/S1063785023900649.
- [17] Y. Foulon, C. Priester, Phys. Rev. B, **45**, 6259 (1992). DOI: 10.1103/PhysRevB.45.6259
- [18] G. Armelles, M.C. Muñoz, M.I. Alonso, Phys. Rev. B, **47**, 16299 (1993). DOI: 10.1103/PhysRevB.47.16299
- [19] A.R. Goni, C. Kristukat, F. Hatami, S. Dresler, W.T. Masselink, C. Thomsen, Phys. Rev. B, **67**, 075306 (2003). DOI: 10.1103/PhysRevB.67.075306

Translated by M.Verenikina